The PedS2/PedR2 two-component system is crucial for the rare earth element switch in *Pseudomonas putida* KT2440

Matthias Wehrmann[a], Charlotte Berthelot[b,c], Patrick Billard[b,c], Janosch Klebensberger[a]#

[a]*University of Stuttgart, Institute of Technical Biochemistry, Stuttgart, Germany*

[b]*Université de Lorraine, LIEC UMR7360, Faculté des Sciences et Technologies, Vandoeuvre-lès-Nancy, France*

[c]*CNRS, LIEC UMR7360, Faculté des Sciences et Technologies, Vandoeuvre-lès-Nancy, France*

Running title: Rare earth element switch in *Pseudomonas putida*

#Address correspondence to Janosch Klebensberger, janosch.klebensberger@itb.uni-stuttgart.de.

Keywords: Lanthanides, rare earth element switch, signalling, *Pseudomonas putida*, PQQ, two-component system, PedS2, PedR2

ABSTRACT

In *Pseudomonas putida* KT2440, two pyrroloquinoline quinone-dependent ethanol dehydrogenases (PQQ-EDHs) are responsible for the periplasmic oxidation of a broad variety of volatile organic compounds (VOCs). Depending on the availability of rare earth elements (REEs) of the lanthanide series (Ln^{3+}), we have recently described that the transcription of the genes encoding the Ca^{2+}-utilizing enzyme PedE and the Ln^{3+}-utilizing enzyme PedH are inversely regulated. With adaptive evolution experiments, site-specific mutations, transcriptional reporter fusions, and complementation approaches, we herein demonstrate that the PedS2/PedR2 (PP_2671/PP_2672) two-component system (TCS) plays a central role in the observed REE-mediated switch of PQQ-EDHs in *P. putida*. We provide evidence that in the absence of lanthanum (La^{3+}), the sensor histidine kinase PedS2 phosphorylates its cognate LuxR-type response regulator PedR2, which in turn not only activates *pedE* gene transcription but is also involved in repression of *pedH*. Our data further suggests that the presence of La^{3+} lowers kinase activity of PedS2, either by the direct binding of the metal ions to the periplasmic region of PedS2 or by an uncharacterized indirect interaction, leading to reduced levels of phosphorylated PedR2. Consequently, the fading *pedE* expression and concomitant alleviation of *pedH* repression causes – in conjunction with the transcriptional activation of the *pedH* gene by a yet unknown regulatory module – the Ln^{3+}-dependent transition from PedE to PedH catalysed oxidation of alcoholic VOCs.

36 # IMPORTANCE

37 The function of lanthanides (Ln^{3+}) for methano- and methylotrophic bacteria is gaining
38 increasing attention, while knowledge about the role of rare earth elements (REEs) in non-
39 methylotrophic bacteria is still limited. The present study investigates the recently described
40 differential expression of the two PQQ-EDHs of *P. putida* in response to Ln^{3+}. We demonstrate
41 that a specific TCS is crucial for their inverse regulation and provide evidence for a dual
42 regulatory function of the LuxR-type response regulator involved. Thus, our study represents
43 the first detailed characterization of the molecular mechanism underlying the REE switch of
44 PQQ-EDHs in a non-methylotrophic bacterium and stimulates subsequent investigations for
45 the identification of additional genes or phenotypic traits that might be co-regulated during
46 REE-dependent niche adaptation.

47 # INTRODUCTION

48 In its natural soil habitat, *Pseudomonas putida* KT2440 is exposed to a broad range of potential
49 carbon and energy sources (Regenhardt *et al.*, 2002; Wackett, 2003; Wu *et al.*, 2011), including
50 plant-, fungi-, or bacterially derived volatile organic compounds (VOCs) with alcohols or
51 aldehydes as functional groups (Insam and Seewald, 2010; Penuelas *et al.*, 2014; van Dam *et*
52 *al.*, 2016). For efficient capture and metabolism of such VOCs, *P. putida* makes use of two
53 PQQ-dependent ethanol dehydrogenases (PQQ-EDHs) – namely PedE and PedH – to carry out
54 the initial oxidation steps in the periplasm of the cell (Mückschel *et al.*, 2012; Wehrmann *et*
55 *al.*, 2017). In a recent study, we found that these two type I quinoproteins (Anthony, 2001;
56 Toyama *et al.*, 2004) exhibit a similar substrate scope, but require different metal cofactors
57 for their catalytic activity (Wehrmann *et al.*, 2017). In contrast to PedE, which uses Ca^{2+} ions,
58 PedH was characterized as a rare earth element (REE)-dependent enzyme that relies on the
59 presence of lanthanide (Ln^{3+}) ions for catalytic activity. Notably, due to their low solubility in
60 most natural environments, REEs have long been considered to have no biological function
61 (Sarkar, 2002). However, the discovery of the wide-spread occurrence of the REE-dependent
62 XoxF-type of PQQ-dependent methanol dehydrogenases (PQQ-MDHs), together with the
63 more recent description of Ln^{3+}-dependent ethanol dehydrogenases, has highlighted the
64 important role of REEs for many bacterial species in various environmental compartments
65 (Fitriyanto *et al.,* 2011a; Fushimi, *et al.*, 2011; Pol *et al.*, 2014; Taubert *et al.*, 2015; Chu and
66 Lidstrom, 2016; Good *et al.*, 2016; Vekeman *et al.*, 2016; Shiller *et al.*, 2017; Wehrmann *et al.*,
67 2017; Lv *et al.*, 2018; Masuda *et al.*, 2018).

68 While in the absence of Ln^{3+} the oxidation of methanol in methylotrophs is driven by Ca^{2+}-
69 dependent PQQ-MDHs (MxaF-type), the presence of low amounts of REE ions is usually
70 sufficient to trigger a transcriptional switch to the XoxF-type of PQQ-MDHs. This inverse

71 regulation, called the REE switch, has been described for many methano- and/or
72 methylotrophic organisms (Farhan Ul Haque *et al.*, 2015; Chu and Lidstrom, 2016; Vu *et al.*,
73 2016; Gu and Semrau, 2017; Masuda *et al.*, 2018; Zheng *et al.*, 2018). From the growing
74 number of studies, it has become apparent that the molecular mechanism underlying this
75 switch for PQQ-MDHs is complex and can substantially differ among species. For example, the
76 inverse regulation in the non-methanotrophic methylotroph *Methylobacterium extorquens*
77 strain AM1 is controlled by two different two-component systems (TCS) (MxcQE and MxbDM)
78 and the orphan response regulator MxaB (Xu *et al.*, 1995; Springer *et al.*, 1997, 1998). In this
79 organism it has been found that the transcriptional activation of both enzymes, the Ca^{2+}-
80 dependent MxaF and the two Ln^{3+}-dependent XoxF1 and XoxF2, is entirely lost in a
81 Δ*xoxF1*Δ*xoxF2* double mutant (Skovran *et al.*, 2011). As a consequence, a complex and
82 consecutive regulation was postulated, in which the different binding affinities of the *apo* (no
83 Ln^{3+} bound to the enzyme) and *holo* (Ln^{3+} bound to the enzyme) form of the XoxF proteins to
84 the periplasmic domain of the sensor histidine kinase MxcQ is essential to regulate the switch
85 (Vu *et al.*, 2016).
86 The type I methanotroph *Methylomicrobium buryatense* strain 5GB1C is lacking homologs of
87 the aforementioned TCS systems MxcQE and MxbDM (Chu and Lidstrom, 2016). In this
88 organism, the REE switch is regulated predominantly by the sensor histidine kinase MxaY (Chu
89 *et al.*, 2016). Chu and coworkers found that the activation of MxaY in the absence of
90 lanthanum activates the transcription of the Ca^{2+}-dependent enzyme MxaF by a so-far
91 unknown response regulator. In addition, the deletion of MxaY was found to almost entirely
92 eliminate the Ln^{3+}-mediated transcriptional activation of the Ln^{3+}-dependent enzyme XoxF in
93 a partially MxaB-dependent manner that also results in a severe growth defect, both in the
94 absence and presence of Ln^{3+}. As an additional layer of complexity, recent studies found that

95 the presence of other metal ions such as copper, which is needed as a cofactor for the
96 membrane-bound or particulate methane monooxygenase (pMMO) in methanotrophs, can
97 significantly impact the REE-mediated switch (Farhan Ul Haque *et al.*, 2015; Gu and Semrau,
98 2017; Semrau *et al.*, 2018).
99 In contrast to the increasing knowledge about the regulation of PQQ-MDHs in methylotrophs,
100 the molecular basis underlying such a regulatory switch for PQQ-EDHs in non-methylotrophic
101 organisms is not established. In the present study, we identify the TCS encoded by
102 PP_2671/PP_2672 (hereinafter referred to as PedS2/PedR2 according to the genetic
103 nomenclature from Arias *et al.*, 2008), consisting of the sensor histidine kinase PedS2 and its
104 cognate LuxR-type transcriptional response regulator PedR2, as an essential regulatory
105 module for the REE-mediated switch of PQQ-EDHs in *P. putida* KT2440. We provide evidence
106 that the activity of PedS2 in the absence of lanthanides leads to phosphorylation of PedR2
107 ($PedR2^P$), which serves a dual regulatory function. On the one hand, $PedR2^P$ acts as a strong
108 transcriptional activator of the *pedE* gene, which is essential to allow growth with 2-
109 phenylethanol in the absence of Ln^{3+}. At the same time, $PedR2^P$ also functions as a repressor
110 of *pedH*. From our data, we conclude that the presence of Ln^{3+} ions triggers a reduction in
111 PedS2 activity, either by a direct binding of the metal to the periplasmic region of PedS2 or by
112 an uncharacterized indirect interaction. This reduction of PedS2 activity, together with a
113 proposed phosphatase activity of PedS2 in its inactivated state, causes the accumulation of
114 non-phosphorylated PedR2, which over-time results in the loss of the regulatory activity of
115 the protein, and facilitates – in concert with the positive feedback function of PedH in the
116 presence of Ln^{3+} ions – the switch between PedE and PedH-dependent growth.

117 # RESULTS

118 ***Identification of the sensor histidine kinase PedS2 as a lanthanide-responsive sensor***

119 As a consequence of the inverse regulation of *pedE* and *pedH*, a *pedH* deletion strain does not
120 grow within 48 h with 2-phenylethanol as sole carbon source in the presence of a critical
121 concentration of La^{3+} in the culture medium (Wehrmann *et al.*, 2017). To test whether strains
122 can be evolved, which are capable of overcoming the repression of *pedE* in the presence of
123 Ln^{3+} ions, an adaptive evolution experiment was performed (see **Figure 1** for a general
124 scheme).

125 When Δ*pedH* cultures were incubated with 2-phenylethanol in the presence of 10 µM La^{3+} ions
126 for longer than 5 d, growth was observed, indicating the occurrence of adapted strains (data
127 not shown). When independent clones were isolated from such cultures and passaged several
128 times on LB agar medium, their growth phenotype with 2-phenylethanol was still much faster
129 (< 2 d) than that observed for their Δ*pedH* parental strain and very similar to the growth
130 phenotype of the wild-type strain KT2440. Similar spontaneous suppressor mutants have been
131 described recently in methylotrophic organisms such as *M. extorquens* strain AM1, *M.*
132 *buryatense strain* 5GB1C, and *M. aquaticum* strain 22A during growth with methanol (Chu and
133 Lidstrom, 2016; Chu *et al.*, 2016; Masuda *et al.*, 2018). In *M. buryatense*, whole genome
134 sequencing revealed that the suppressor mutant strain was characterized by a mutation in the
135 membrane bound two-component sensor histidine kinase MxaY (Chu *et al.*, 2016). In *P. putida*
136 KT2440, the gene PP_2671 (hereinafter referred to as *pedS2*), located in close genomic
137 proximity to *pedE* (PP_2674), encodes a membrane bound histidine kinase sharing 25 % amino
138 acid sequence identity with MxaY (**Figure 1D-F**). To test the hypothesis that mutations in
139 *pedS2* are responsible for the emergence of suppressor phenotypes in strain Δ*pedH* during
140 growth in the presence of La^{3+}, the gene was sequenced in three individually isolated mutants

141 (Δ*pedH*$^{S1-3}$) (**Figure 1A-D**). This analysis revealed that all strains contained a mutation in the
142 *pedS2* sequence leading to a non-synonymous substitution. These mutations were either
143 located within a predicted periplasmic domain of unknown function (R73C [Δ*pedH*^{S1}] and
144 R111W [Δ*pedH*^{S2}]) or within the HAMP domain (S178P [Δ*pedH*^{S3}]), which is responsible for
145 signal transduction from the periplasm into the cytoplasm of the cell (Stock *et al.*, 2000;
146 Parkinson, 2010). To verify that the identified mutations in *pedS2* are the primary cause of the
147 suppressor phenotype, the S178P mutation from Δ*pedH*^{S3} was introduced into the genetic
148 background of strain Δ*pedH*, resulting in strain Δ*pedH*_PedS^{S178P}.
149 In subsequent growth experiments with 2-phenylethanol in the absence of La^{3+}, strains Δ*pedH*
150 and Δ*pedH*_PedS2^{S178P} showed a similar growth behavior with a lag phase of < 32 h (**Figure**
151 **2A1**; **Figure 2A2**). In the presence of 10 µM La^{3+}, however, Δ*pedH* showed no growth within
152 72 h, whereas Δ*pedH*_PedS2^{S178P} reached its maximum optical densities again after about 32
153 h of incubation, verifying that the observed mutation in the histidine kinase *pedS2* was
154 sufficient to cause the suppressor phenotype. We speculated that the LuxR-type response
155 regulator PP_2672 (hereinafter referred to as *pedR2*), which is located adjacent to *pedS2*
156 within the genome of *P. putida* KT2440, represents the target of PedS2 activity. This
157 assumption is based on the fact that PedR2 represents a homologue (65% amino acid
158 sequence identity) of EraR (ExaE; PA1980), which forms a TCS with the cytosolic histidine
159 kinase EraS (ExaD; PA1979) that activates expression of the *pedE* homologue *exaA* in
160 *Pseudomonas aeruginosa* (Schobert and Görisch, 2001; Mern *et al.*, 2010). To test this
161 hypothesis, *pedS2* as well as its potential cognate response regulator encoding gene *pedR2*,
162 were deleted in a Δ*pedH* background. In addition, strains suitable for probing promoter
163 activity of *pedE* in strains Δ*pedH,* Δ*pedH*_PedS2^{S178P}, Δ*pedH*Δ*pedS2* and Δ*pedH*Δ*pedR2* were

164 constructed and subsequently analyzed during growth with 2-phenylethanol in the presence
165 and absence of La^{3+} (**Figure 2B**).

166 ***The TCS PedS2/PedR2 regulates pedE transcription in response to lanthanide availability***

167 In accordance with the observed growth patterns, *pedE* promoter activities in strain
168 Δ*pedH*_PedS2^{S178P} were almost identical in both the absence and the presence of La^{3+} (ratio
169 no La^{3+} to 1 µM La^{3+}: 0.89 ± 0.02) but increased more than 24-fold (24 ± 1 and 27 ± 1-fold,
170 respectively) compared to the *pedE* promoter activities determined for cells of strain Δ*pedH*
171 in the absence of La^{3+} (**Figure 2B**). Strain Δ*pedH*Δ*pedS2* also showed a La^{3+}-independent
172 growth phenotype similar to strain Δ*pedH*_PedS2^{S178P}, however with a clear delay (< 48 h vs.
173 < 32 h) (**Figure 2A3**). Promoter activities for *pedE* were almost identical in this strain in the
174 absence and presence of La^{3+} (ratio no La^{3+} to 1 µM La^{3+}: 1.07 ± 0.09) (**Figure 2B**).
175 In contrast, incubations of 72 h (**Figure 2A4**) or even prolonged incubations for more than 7 d
176 (data not shown) did not result in detectable growth of strain Δ*pedH*Δ*pedR2* with 2-
177 phenylethanol, both in the presence and absence of La^{3+}. Correspondingly, *pedE* promoter
178 activities in this strain were low compared to those observed for cells of strain Δ*pedH* in the
179 presence of La^{3+} but in a similar range as those observed for Δ*pedH*Δ*pedS2* in the presence
180 and absence of La^{3+}. These data demonstrate that the PedS2/PedR2 system is the
181 predominant element in the La^{3+}-dependent regulation of *pedE* and that PedR2 is essential for
182 PedE-dependent growth. However, as PedE-dependent growth can still be observed in the
183 absence of PedS2 after prolonged incubations and in a PedR2-dependent manner (**Figure 2A3;**
184 **Figure 2A4**), we assume that at least one additional lanthanide-independent kinase must be
185 able to phosphorylate PedR2, leading to transcriptional activation of *pedE* and functional
186 production of the calcium-dependent enzyme under these conditions.

187 ***The TCS PedS2/PedR2 regulates the partial repression of pedH in the absence of lanthanides***

188 Based on the critical role of PedS2/PedR2 in the regulation of *pedE* and the fact that LuxR-type
189 regulators have been demonstrated to be capable of acting as both transcriptional activators
190 and repressors (Waters and Bassler, 2006; Van Kessel *et al.*, 2013), we speculated that this
191 TCS could also be involved in the regulation of *pedH*. To test this hypothesis, strains
192 Δ*pedE*_PedS2^{S178P}, Δ*pedE*Δ*pedS2*, and Δ*pedE*Δ*pedR2* were generated and a transcriptional
193 reporter suitable for probing *pedH* promoter activities was integrated into the genome of each
194 of these strains.
195 Experiments with 2-phenylethanol revealed that strains Δ*pedE*, Δ*pedE*Δ*pedS2*, and
196 Δ*pedE*Δ*pedR2* showed La^{3+}-dependent growth after a lag-phase < 24 h and reached the
197 maximum OD_{600} after ≤ 32 h **(Figure 3A1**; **Figure 3A3**; **Figure 3A4**). In contrast, strain
198 Δ*pedE*_PedS2^{S178P} exhibited an extended lag-phase (> 24 h) and consistently reached the
199 maximal OD_{600} only after prolonged incubations (≥ 32 h; **Figure 3A2**). In accordance with these
200 growth results, *pedH* promoter activities of strains Δ*pedE*, Δ*pedE*Δ*pedS2,* and Δ*pedE*Δ*pedR2*
201 were in a similar range, whereas *pedH* promoter activities in strain Δ*pedE*_PedS2^{S178P} were 45
202 ± 2-fold and 30 ± 2-fold lower than strain Δ*pedE* in absence or presence of La^{3+}, respectively
203 (**Figure 3B**). Assuming that the S178P mutation in PedS2 results in a sensor kinase activity that
204 mimics that of the wild-type protein in the absence of lanthanides, it is very likely that PedS2
205 is responsible for the repression of *pedH* under the La^{3+}-free conditions leading to the
206 observed delay in growth. To find out whether this regulatory effect on *pedH* proceeds *via* the
207 response regulator PedR2, as it is the case for *pedE*, or is caused by an unknown additional
208 target of PedS2, the triple mutant strain Δ*pedE*_PedS2^{S178P}Δ*pedR2* was generated and
209 characterized for its growth phenotype (**Figure 4A**). In this experiment, Δ*pedE* and
210 Δ*pedE*_PedS2^{S178P} both grew with 2-phenylethanol, however, with a clear difference in the
211 corresponding lag-phases confirming the previous results from growth in 96-well plates

212 (**Figure 3A**). In contrast, the additional deletion of the response regulator PedR2 eliminated
213 the growth defect caused by the PedS2^{S178P} allele, leading to a growth behavior of
214 Δ*pedE*_PedS2^{S178P}Δ*pedR2* (**Figure 4A**), which was indistinguishable from that of strain Δ*pedE*.

215 **The conserved phosphorylation site D53 in PedR2 is essential for the REE-mediated switch**

216 In order to study the essentiality of the phosphorylation site at position D53 of PedR2 (Bourret
217 *et al.*, 1990; Milani *et al.*, 2005), we used inducible constructs for the production of the wild-
218 type PedR2 protein (pJEM[PedR2]) and a mutated variant, in which the conserved aspartate
219 in the CheY-like receiver domain was replaced by an alanine (pJEM[PedR2^{D53A}]). After
220 transformation of these plasmids into strains Δ*pedH*Δ*pedR2* and Δ*pedE*_PedS2^{S178P}Δ*pedR2*
221 their growth with 2-phenylethanol in the absence and presence of La^{3+} was monitored. When
222 the plasmid-borne wild-type regulator PedR2 was induced in cells of
223 Δ*pedH*_PedS2^{S178P}Δ*pedR2,* growth was observed after a lag-phase of < 24 h whereas the
224 PedR2^{D53A} variant was unable to restore PedE-dependent growth in the same strain (**Figure**
225 **4B**). Intriguingly, the reverse result was obtained in strain Δ*pedE*_PedS2^{S178P}Δ*pedR2*. Here, the
226 PedR2^{D53A} variant allowed PedH-dependent growth, whereas the wild-type regulator PedR2
227 did not lead to significant growth within 120 h of incubation (**Figure 4C**).

228 # DISCUSSION

229 We recently demonstrated that in *P. putida* KT2440 the production of the two PQQ-EDHs PedE
230 and PedH is both tightly and inversely regulated depending on lanthanide availability,
231 representing the first reported REE switch for PQQ-EDHs in a non-methylotrophic organism
232 (Wehrmann *et al.*, 2017). While we were able to show that Ln^{3+}-dependent transcriptional
233 activation of *pedH* is mostly, but not entirely, dependent on the presence of the PedH protein
234 itself, the Ln^{3+}-dependent transcriptional repression of *pedE* remained elusive. In this study,
235 we present a detailed characterization of the mechanism underlying PedE and PedH
236 regulation (**Figure 5**), in which the TCS PedS2/PedR2 acts as an essential signaling module for
237 the REE-mediated switch between the two quinoproteins. Similar to the recently
238 characterized spontaneous mutant of *M. buryatense* (Chu *et al.*, 2016), we found that a single
239 non-synonymous mutation within the periplasmic region of the sensor histidine kinase PedS2
240 ($PedS2^{S178P}$), which differs from the LapD/MoxY domain found in MxaY of *M. buryatense*
241 (**Figure 1**), is sufficient to terminate the Ln^{3+}-mediated repression of *pedE*. Notably, various
242 mutations at different sites of the protein can cause the observed suppressor phenotype. This
243 might explain the repeatedly and fast occurrence of these suppressor mutants in our
244 experiments and would support a similar notion in *M. buryatense* (Chu and Lidstrom, 2016;
245 Chu *et al.*, 2016).

246 Besides the essentiality for *pedE* regulation, our experimental data further provide strong
247 evidence that PedS2 is also involved in the repression of *pedH* in the absence of lanthanides,
248 but not in its Ln^{3+}-dependent activation. This is based on the observation that the
249 Δ*pedE*Δ*pedS2* deletion strain did not show any differences in growth and *pedH* regulation,
250 while the suppressor mutant Δ*pedE*_$PedS2^{S178P}$ displayed decreased *pedH* promoter activity
251 and a strongly increased lag-phase in growth experiments in the presence of La^{3+}. We

252 additionally show that the *pedS2*-dependent regulations of *pedE* and *pedH* are both mediated
253 by the LuxR-type response regulator PedR2. From these data we conclude that in absence of
254 La^{3+} ions the PedS2 sensor histidine kinase is active and triggers phosphorylation of PedR2 at
255 the conserved position D53 ($PedR2^{P}$) (Bourret *et al.*, 1990; Milani *et al.*, 2005). The
256 phosphorylated state of PedS2 subsequently has a dual regulatory function, namely the
257 activation of *pedE* and concomitant repression of *pedH* transcription (**Figure 5A**). In this
258 context, it is interesting to note that expression of the gene *exaA* in *Azospirillum brasilense*
259 Sp7, which encodes for a PQQ-dependent alcohol dehydrogenase, is dependent on σ^{54} and its
260 interaction with a LuxR-type response regulator that shares 45% sequence identity with PedR2
261 (Singh *et al.*, 2017). Whether the transcriptional activation of *pedE* is dependent on a similar
262 interaction of PedR2 with a specific sigma factor is currently unknown.
263 To our surprise, also a Δ*pedH*Δ*pedS2* mutant was able to grow on 2-phenylethanol, even
264 though with an increased lag-phase and low *pedE* promoter activities (**Figure 2A3**). This
265 indicates that at least one additional kinase beside PedS2 must be capable of phosphorylating
266 PedR2 to facilitate growth of this strain under these conditions. Given that such an additional
267 kinase exists, it is surprising that a *pedH* single mutant, in contrast to the aforementioned
268 Δ*pedH*Δ*pedS2* double mutant, is only able to grow in the presence of REEs when PedS2 is
269 mutated (e.g. $PedS2^{S178P}$; **Figure 2A1)**. This suggests that the activity of the additional, non-
270 specific histidine kinase towards PedR2 in the presence of La^{3+} is repressed as long as PedS2
271 is functional. We hence propose that PedS2, as many other sensory histidine kinases in
272 bacteria (Stock *et al.*, 2000; Rowland and Deeds, 2014; Agrawal *et al.*, 2016), also exhibits
273 phosphatase activity on $PedR2^{P}$ in the presence of La^{3+}, thereby ensuring specificity of the
274 signal transduction pathway and eliminating the interference from other non-specific kinases.
275 In our working hypothesis, the presence of lanthanides in the medium leads to the repression

276 of PedS2 kinase activity, most likely by direct binding of the metal ions to its periplasmic
277 domain (**Figure 5B**). The reduced kinase- and postulated phosphatase activity of PedS2
278 consequently leads to the accumulation of unphosphorylated PedR2, which finally results in
279 the loss of its regulatory functions. In addition, the transcription of *pedH* is activated *via* a yet
280 unknown pathway, in which a functional PedH protein is an essential component most likely
281 by acting as a lanthanide sensor (Wehrmann *et al.*, 2017).
282 In conclusion, it appears that the REE-mediated switches in *M. extorquens* AM1 and *M.*
283 *buryatense* during growth with methanol are predominantly dependent on only one
284 lanthanide responsive pathway, which either proceeds via the XoxF1 and XoxF2 proteins or
285 MxaY (Chu *et al.*, 2016; Vu *et al.*, 2016). Our results establish that in *P. putida* KT2440, a
286 combination of at least two independent pathways are important to orchestrate the inverse
287 regulation of *pedE* and *pedH* in response to lanthanides efficiently.
288 Several recent studies suggest that in methano- and methylotrophic bacteria, the REE switch
289 might affect more genes than only those needed for the periplasmic oxidation system itself
290 (Gu and Semrau, 2017; Good *et al.*, 2018; Masuda *et al.*, 2018). Reports on physiological
291 consequences are, however, inconsistent as some studies found no effects (Nakagawa *et al.*,
292 2012; Chu and Lidstrom, 2016; Vu *et al.*, 2016; Masuda *et al.*, 2018), whereas other studies
293 reported a stimulating effect on biofilm formation, growth rates, and overall yields in the
294 presence of REE (Fitriyanto *et al.*, 2011b; Nakamura, *et al.*, 2011; Good *et al.*, 2018). We think
295 it is not unlikely that additional REE-mediated regulatory effects do also exist in *P. putida*
296 KT2440 in a context-dependent manner. Thus, one of our current foci is to investigate the
297 global regulatory impact and physiological consequences of the presence and absence of
298 lanthanides under varying environmental conditions.

299 # MATERIAL AND METHODS

300 ***Bacterial strains, plasmids and culture conditions***

301 A detailed description of the strains and plasmids used in this study can be found in **Table 1**.
302 If not stated otherwise *Escherichia coli* and *P. putida* KT2440 strains were maintained on
303 solidified LB medium. Routinely, strains were cultured in liquid LB medium (Maniatis *et al.*,
304 1982) or a modified M9 salt medium (Wehrmann *et al.*, 2017) supplemented with 25 mM
305 succinate or 5 mM 2-phenylethanol as source of carbon and energy at 30°C and shaking, if not
306 stated otherwise. For maintenance and selection, 40 µg mL^{-1} kanamycin or 15 µg mL^{-1}
307 gentamycin for *E.coli* and 40 µg mL^{-1} kanamycin, 20 µg mL^{-1} 5-fluoro uracil, or 15 µg mL^{-1}
308 gentamycin for *P. putida* strains was added to the medium, if indicated.

309 ***Liquid medium growth experiments***

310 All liquid growth experiments were carried out using modified M9 with 25 mM succinate or 5
311 mM 2-phenylethanol as sole source of carbon and energy (see above) in 125 ml or 250 ml
312 polycarbonate Erlenmeyer flask (Corning) or in 96-well 2 ml deep-well plates (Carl Roth), as
313 described previously (Wehrmann *et al.*, 2017). Briefly, washed cells from overnight cultures
314 grown with succinate at 30°C and 180 rpm shaking were used to inoculate fresh medium with
315 an OD_{600} of 0.01 and incubated at 30°C and 180 rpm (growth experiments in polycarbonate
316 Erlenmeyer flasks) or 350 rpm (growth experiments in 96-well plates) shaking.

317 ***Construction of plasmids***

318 For construction of the deletion plasmids pMW55, pMW56 and pMW61 the 600 bp regions
319 upstream and downstream of gene *pedS2* (*PP_2671*), amino acid residue S178 in gene *pedS2*
320 (*PP_2671*), or gene *pedR2* (*PP_2672*) were amplified from genomic DNA of *P. putida* KT2440
321 using primers MWH90-93, MWH98-101 or MWH106-109 (**Table 1**). The two up- and

322 downstream fragments and BamHI digested pJOE6261.2 were then joined together using one-
323 step isothermal assembly (Gibson, 2011). Upon subsequent transformation of the constructs
324 into *E. coli* BL21(DE3) cells, the correctness of the plasmids was confirmed by Sanger
325 sequencing. Plasmids pJeM[pedR2] and pJEM[PedR2^{D53A}] encoding for PedR2 or PedR2 with
326 mutated amino acid residue 53 (D→A) under a rhamnose inducible promoter were ordered
327 from an external source (Eurofins).

328 ***Strain constructions and isolation of suppressor mutants***

329 The *pedS2* (*PP_2671*) and *pedR2* (*PP_2672*) negative mutants as well as the PedS2^{S178P} allele
330 were constructed using a recently described system for markerless gene deletion in *P. putida*
331 KT2440 (Graf and Altenbuchner, 2011). Briefly, the integration vectors harboring the up- and
332 downstream regions of the target genes (pMW55 and pMW61) or the up- and downstream
333 regions of the region to be mutated including the desired S178P mutation (pMW56) were
334 transformed into *P. putida* KT2440* and kanamycin (Kan) resistant and 5-flourouracil (5-FU)
335 sensitive clones were selected on LB Kan agarose plates. After incubation at 30°C for 24 h in
336 LB medium without selection markers, clones that were 5-FU^{R} and Kan^{S} were tested for
337 successful gene deletion using primer pair MWH90/MWH93 or MWH106/MWH109 for gene
338 *pedS2* or *pedR2*, respectively. The presence of the underlying PedS2^{S178P} mutation was verified
339 by Sanger sequencing after gene *pedS2* of 5-FU^{R} and Kan^{S} clones was amplified using primer
340 pair MWH85/MWH86. Δ*pedH* suppressor mutant strains were isolated from 25 ml liquid M9
341 cultures with 5 mM 2-phenylethanol as sole source of carbon and energy supplemented with
342 10 µM La^{3+} upon > 5 d incubation at 30°C and 180 rpm. Strains were passed thrice over LB agar
343 plates and reevaluated for growth in liquid M9 medium supplemented with 5 mM 2-
344 phenylethanol and 10 µM La^{3+}. From cultures that showed growth upon a similar lag-phase as

345 the KT2440* wild-type strain, the *pedS2* gene was amplified by PCR using primer pair
346 M85/M86 and mutations were identified by Sanger sequencing.
347 To construct reporter strains for the analysis of *pedE* and *pedH* promoter activity in different
348 genetic backgrounds, plasmids pUC18-mini-Tn*7*T-*pedE-lux-Gm* and pUC18-mini-Tn*7*T-*pedH-*
349 *lux-Gm* (Wehrmann *et al.*, 2017) were co-electroporated with the helper plasmid pTNS2 into
350 selected mutant strains of *P. putida* KT2440 (**Table 1**). Proper chromosomal integration of the
351 mini-Tn7 element in gentamycin resistant transformants was verified by colony PCR using P_{put-}
352 $_{glmS}$DN and P_{Tn7R} primers as described previously (Choi *et al.*, 2005).

353 ***Reporter gene fusion assays***

354 For quantitative measurement of *pedE* and *pedH* promoter activity, strains of *P. putida*
355 harboring a Tn*7*-based *pedE-lux* or *pedH-lux* transcriptional reporter fusion were grown
356 overnight in LB medium with gentamycin (15 µg.ml^{-1}), diluted to an OD_{600} = 0.2 in fresh LB
357 medium and grown to an OD_{600} of 0.6. Cells were then washed three times in M9 medium
358 without carbon source and finally adjusted to an OD_{600} of 0.2 in M9 medium with 1 mM 2-
359 phenylethanol. For luminescence measurements, 198 µl of cell suspension was added to 2 µl
360 of a 100 µM $LaCl_3$ solution in white 96-well plates with a clear bottom (µClear; Greiner Bio-
361 One). Microtiter plates were placed in a humid box to prevent evaporation and incubated at
362 28°C with continuous agitation (180 rpm), and light emission and OD_{600} were recorded at
363 regular intervals in an FLX-Xenius plate reader (SAFAS, Monaco) for 6 h. For both parameters,
364 the background provided by the M9 medium was subtracted and the luminescence was
365 normalized to the corresponding OD_{600}. Experiments were performed with biological
366 triplicates, and data are presented as the mean value with error bars representing the
367 corresponding standard deviation.

368 ***Sequence identity determination***

Protein sequence identities were determined based on amino acid sequence alignments of the proteins of interest generated using the Clustal Omega multiple sequence alignment tool (Sievers *et al.*, 2014).

FUNDING INFORMATION

The work of Matthias Wehrmann and Janosch Klebensberger was supported by an individual research grant from the Deutsche Forschungsgemeinschaft (DFG, KL 2340/2-1). The work of Charlotte Berthelot and Patrick Billard was supported in part by Labex Ressources21 (ANR-10-LABX-21-01).

ACKNOWLEDGEMENTS

The authors would like to thank Prof. Bernhard Hauer for his continuous support. The authors further declare that the research was conducted in the absence of any commercial or financial relationships that could be construed as a potential conflict of interest.

381 # Tables

382 **Table 1:** Strain, plasmids, and primer used in the study

Strains	**Relevant features**
KT2440	Wild-type strain of *Pseudomonas putida* (ATCC 47054)
KT2440*	KT2440 with a markerless deletion of *upp* | Parent strain for deletion mutants (Graf and Altenbuchner, 2011)
Δ*pedE*	KT2440* with a markerless deletion of *pedE* (Mückschel *et al.*, 2012)
Δ*pedE*Δ*pedS2*	Δ*pedE* with a markerless deletion of *pedS2* (*PP_2671*) (this study)
Δ*pedE*Δ*pedR2*	Δ*pedE* with a markerless deletion of *pedR2* (*PP_2672*) (this study)
Δ*pedE*_PedS2^{S178P}	Δ*pedE* with S178P mutation in PedS2 (this study)
Δ*pedE*_PedS2^{S178P}Δ*pedR2*	Δ*pedE*_PedS2^{S178P} with a markerless deletion of *pedR2* (this study)
Δ*pedH*	KT2440* with a markerless deletion of *pedH* (Mückschel *et al.*, 2012)
Δ*pedH*Δ*pedS2*	Δ*pedH* with a markerless deletion of *pedS2* (this study)
Δ*pedH*Δ*pedR2*	Δ*pedH* with a markerless deletion of *pedR2* (this study)
Δ*pedH*_PedS2^{S178P}	Δ*pedH* with S178P mutation PedS2 (this study)
Δ*pedH*_PedS2^{S178P}Δ*pedR2*	Δ*pedH*_PedS2^{S178P} with a markerless deletion of *pedR2* (this study)
E. coli BL21 (DE3)	*F^- ompT gal dcm lon hsdS$_B$(r_B^- m_B^-) λ(DE3 [lacI lacUV5-T7 gene 1 ind1 sam7 nin5])*
E. coli DH5α	*fhuA2 lac(del)U169 phoA glnV44 Φ80' lacZ(del)M15 gyrA96 recA1 relA1 endA1 thi-1 hsdR17*
KT2440*::Tn7-*pedE-lux*	KT2440* with insertion of miniTn7-*pedE-lux* (Wehrmann *et al.*, 2017)
KT2440*::Tn7-pedH-lux	KT2440* with insertion of miniTn7-*pedH*-lux (Wehrmann et al., 2017)
Δ*pedE*::Tn7-*pedE-lux*	Δ*pedE* with insertion of miniTn7-*pedE-lux* (Wehrmann *et al.*, 2017)
Δ*pedE*::Tn7-*pedH-lux*	Δ*pedE* with insertion of miniTn7-*pedH-lux* (Wehrmann *et al.*, 2017)
Δ*pedH*::Tn7-*pedE-lux*	Δ*pedH* with insertion of miniTn7-*pedE-lux* (Wehrmann *et al.*, 2017)
Δ*pedH* ::Tn7-*pedH-lux*	Δ*pedH* with insertion of miniTn7-*pedH-lux* (Wehrmann *et al.*, 2017)
Δ*pedE*Δ*pedS2*::Tn7-*pedH-lux*	Δ*pedE*Δ*pedS2* with insertion of miniTn7-*pedH-lux* (this study)
Δ*pedE*Δ*pedR2*::Tn7-*pedH-lux*	Δ*pedE*Δ*pedR2* with insertion of miniTn7-*pedH-lux* (this study)
Δ*pedE*_PedS2^{S178P} ::Tn7-*pedH-lux*	Δ*pedE*_PedS2^{S178P} with insertion of miniTn7-*pedH-lux* (this study)
Δ*pedH*Δ*pedS2*::Tn7-*pedE-lux*	Δ*pedH*Δ*pedS2* with insertion of miniTn7-*pedE-lux* (this study)
Δ*pedH*Δ*pedR2*::Tn7-*pedE-lux*	Δ*pedH*Δ*pedR2* with insertion of miniTn7-*pedE-lux* (this study)
Δ*pedH*_PedS2^{S178P} ::Tn7-*pedE-lux*	Δ*pedH*_PedS2^{S178P} with insertion of miniTn7-*pedE-lux* (this study)
Plasmids	
pJeM1	Rhamnose inducible vector (Jeske and Altenbuchner, 2010)
pJOE6261.2	Suicide vector for gene deletions (Graf and Altenbuchner, 2011)
pMW55	pJOE6261.2 based deletion vector for gene *PP_2671* (this study)
pMW56	pJOE6261.2 based vector for introducing the S178P mutation in PedS2 (this study)
pMW61	pJOE6261.2 based deletion vector for gene *PP_2672* (this study)
pUC18-mini-Tn*7*T-*pedE-lux-Gm*	pUC18-mini-Tn*7*T-Gm-lux vector with the promoter of *pedE* driving transcription of *luxCDABE* (Wehrmann *et al.*, 2017)

pUC18-mini-Tn*7*T-*pedH*-*lux*-Gm	pUC18-mini-Tn*7*T-*lux*-Gm vector with the promoter of *pedH* driving transcription of *luxCDABE* (Wehrmann *et al.*, 2017)	
pTNS2	Helper plasmid for Tn7 integration (Choi *et al.*, 2005)	
pJEM[PedR2]	Rhamnose inducible induction of PedR2 (this study)	
pJEM[PedR2^{D53A}]	Rhamnose inducible induction of PedR2^{D53A} (this study)	
Primer		
Name	**Sequence 5' → 3'**	**Annealing**
MWH85	GGAAATATGCAGAAAGTAGCGCTCG	60°C
MWH86	TCTTCACCACTGGCGGCCT	60°C
MWH90	GCCGCTTTGGTCCCGCAGGCACTGGCTGCTGC	60°C
MWH91	CGATATTCAAAGCGGTTCTCCTCAGGC	60°C
MWH92	GAACCGCTTTGAATATCGTGTTGGTCGATGACCAC	60°C
MWH93	GCAGGTCGACTCTAGAGGATGCACAAGCTCGGCG	60°C
MWH98	GCCGCTTTGGTCCCGAGGTAGTAATTCAGTGCGGGGG	60°C
MWH99	TGCCCGCCTGGGACCTGGTG	60°C
MWH100	GGTCCCAGGCGGGCAATTG	60°C
MWH101	GCAGGTCGACTCTAGAGGCAGCCATTGTCGCGAATG	60°C
MWH106	GCCGCTTTGGTCCCGGCAGGAGCAGGAGCGTAC	65°C
MWH107	TGAAATACCCACACCTCCTGGGGAATGTTAAG	65°C
MWH108	GGAGGTGTGGGTATTTCATTGCACCTGTTGGGGC	65°C
MWH109	GCAGGTCGACTCTAGAGGAGCCAACCTGACCC	65°C

383

384 # Figures

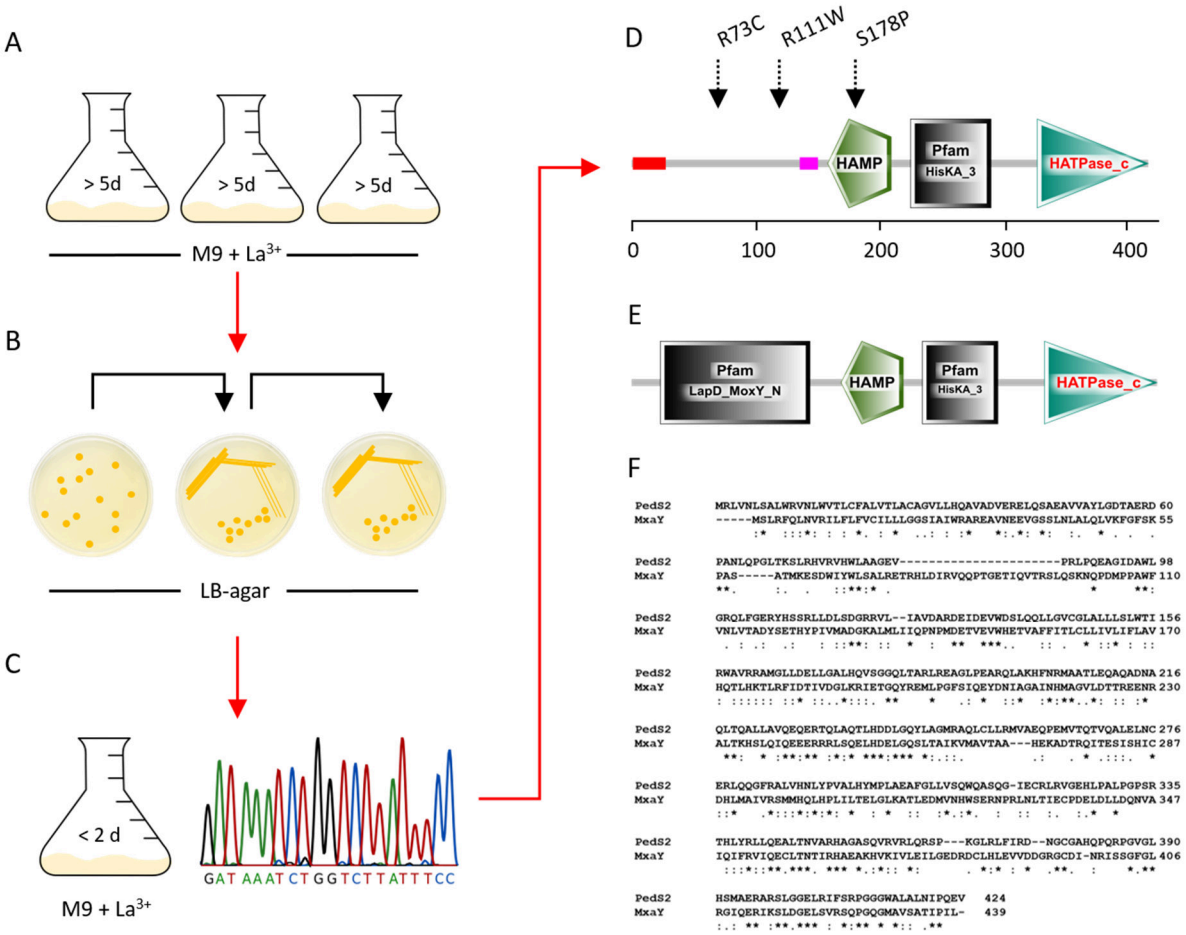

385

386 **Figure 1:** Scheme of selection (**A**), clonal isolation (**B**), characterization and single nucleotide
387 polymorphism (SNP) identification (**C-D**) in the two-component sensor histidine kinase PedS2
388 of the spontaneous mutants Δ*pedH*^{S1} (R73C), Δ*pedH*^{S2} (R111W), Δ*pedH*^{S3} (S178P). **A**) Cells of
389 strain Δ*pedH* were incubated in M9 medium supplemented with 5 mM 2-phenylethanol and
390 10 µM $LaCl_3$ in plastic Erlenmeyer flasks (n = 3) at 30°C with shaking at 180 rpm. **B**) After growth
391 was observed (> 5 days), dilutions from each culture were plated onto LB-agar plates and
392 incubated at 30°C. Individual clones were further streaked on LB-agar twice prior to further
393 characterization. **C**) Clones were characterized for their growth behavior in M9 medium with
394 5 mM 2-phenylethanol in the presence of 10 µM $LaCl_3$. Subsequently, one clone from each
395 culture exhibiting faster growth than the parental strain Δ*pedH* was used for PCR amplification

396 of the *pedS2* gene and multi sequence alignment analysis with the native sequence of the
397 gene from the *Pseudomonas* Genome Database (Winsor *et al.*, 2016). **D-E**) Visualization of
398 domain composition of PedS2 of *P. putida* (**D**) and MxaY of *M. buryatense* 5GB1C (**E**) using the
399 prediction from the Simple Modular Architecture Research Tool (Letunic and Bork, 2018). **F**)
400 Amino acid sequence alignment of the PedS2 and MxaY proteins generated with Clustal
401 Omega (Sievers *et al.*, 2014).

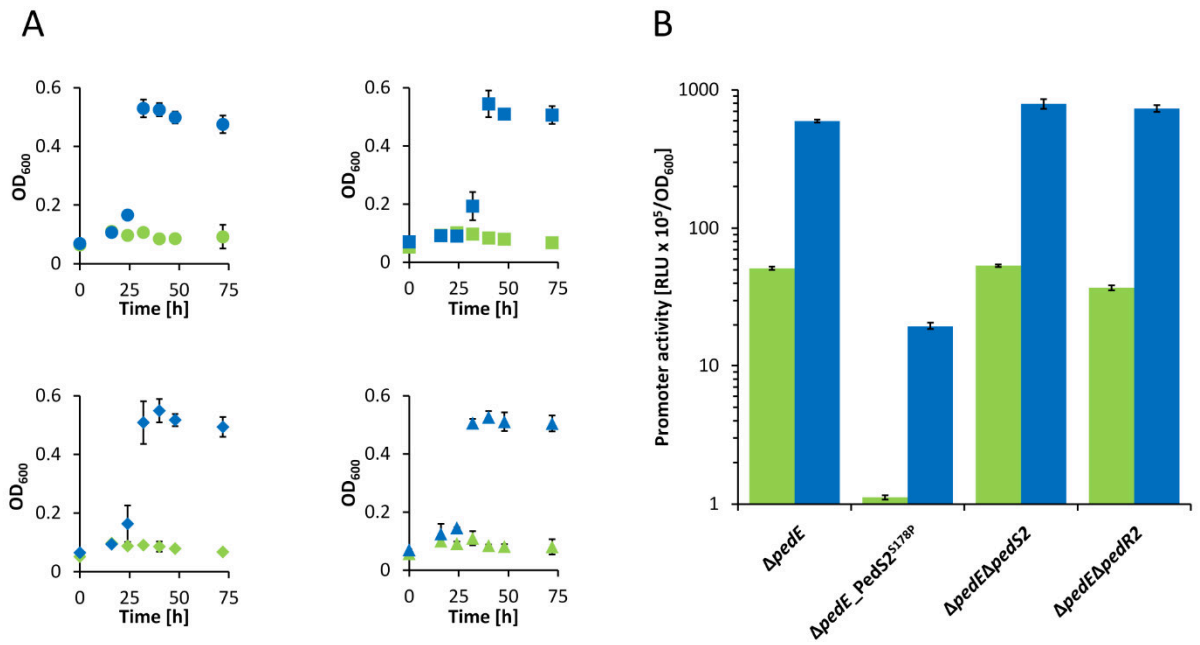

402

403 **Figure 2:** (**A**) Growth of strains Δ*pedH* (circles; 1), Δ*pedH_pedS2*^{S178P} (squares; 2),
404 Δ*pedH*Δ*pedS2* (diamonds; 3), and Δ*pedH*Δ*pedR2* (triangles; 4) at 30°C and 350 rpm shaking
405 with M9 medium in 96-well plates supplemented with 5 mM 2-phenylethanol in absence
406 (green symbols) or presence (blue symbols) of 10 µM La^{3+}. The grey area visualizes the time
407 point by which the parental strain Δ*pedH* (circles) reached an OD_{600} > 0.4 (dotted line) (**B**)
408 Activities of the *pedE* promoter in strains Δ*pedH,* Δ*pedH*_PedS2^{S178P}*,* Δ*pedH*Δ*pedS2,* and
409 Δ*pedH*Δ*pedR2* in the absence (green bars) or presence (blue bars) of 1 µM La^{3+} measured in
410 M9 medium supplemented with 1 mM 2-phenylethanol. Promoter activities are presented in
411 relative light units (RLU x 10^4) normalized to OD_{600}. All data represent the mean of biological
412 triplicates and error bars correspond to the respective standard deviations.

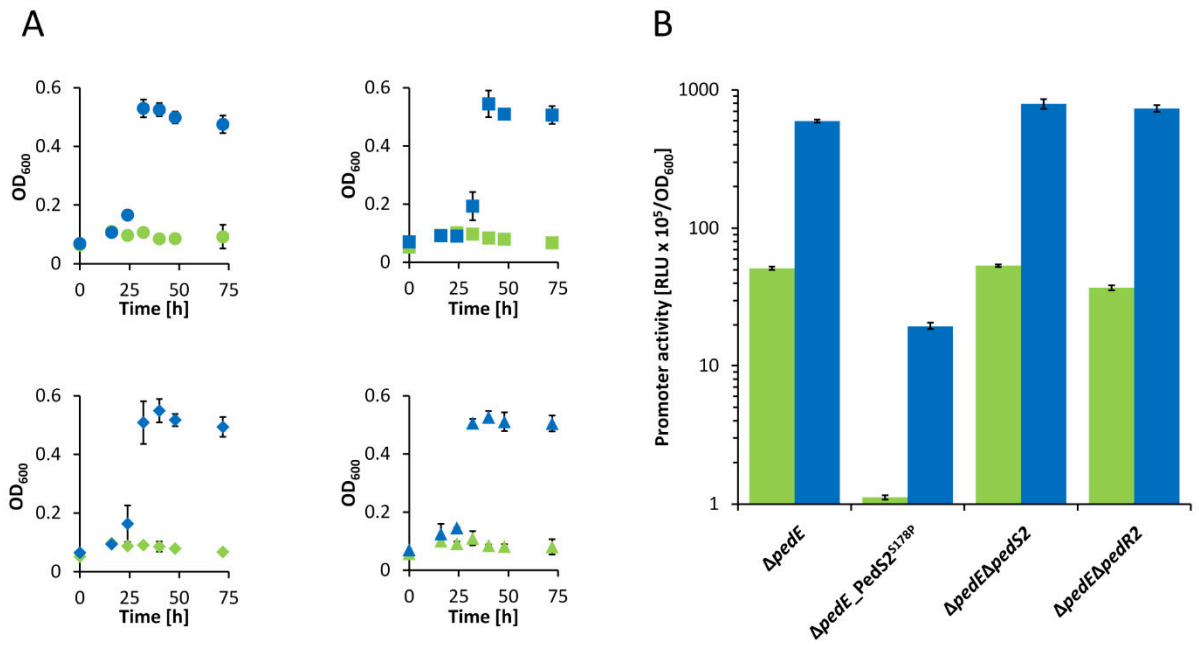

Figure 3: (**A**) Growth of strains Δ*pedE* (circles; 1), Δ*pedE*_PedS2^{S178P} (squares; 2), Δ*pedE*Δ*pedS2* (diamonds; 3), and Δ*pedE*Δ*pedR2* (triangles; 4) at 30°C and 350 rpm shaking with M9 medium in 96-well plates supplemented with 5 mM 2-phenylethanol in absence (green symbols) or presence (blue symbols) of 10 µM La^{3+}. The grey area visualizes the time point by which the parental strain Δ*pedE* (circles) reached their maximum OD_{600} (**B**) Activities of the *pedH* promoter in strains Δ*pedE,* Δ*pedE*_PedS2^{S178P}*,* Δ*pedE*Δ*pedS2,* and Δ*pedE*Δ*pedR2* in the absence (green bars) or presence (blue bars) of 1 µM La^{3+} measured in M9 medium supplemented with 1 mM 2-phenylethanol. Promoter activities are presented in relative light units (RLU x 10^5) normalized to OD_{600}. All data represent the mean of biological triplicates and error bars correspond to the respective standard deviations.

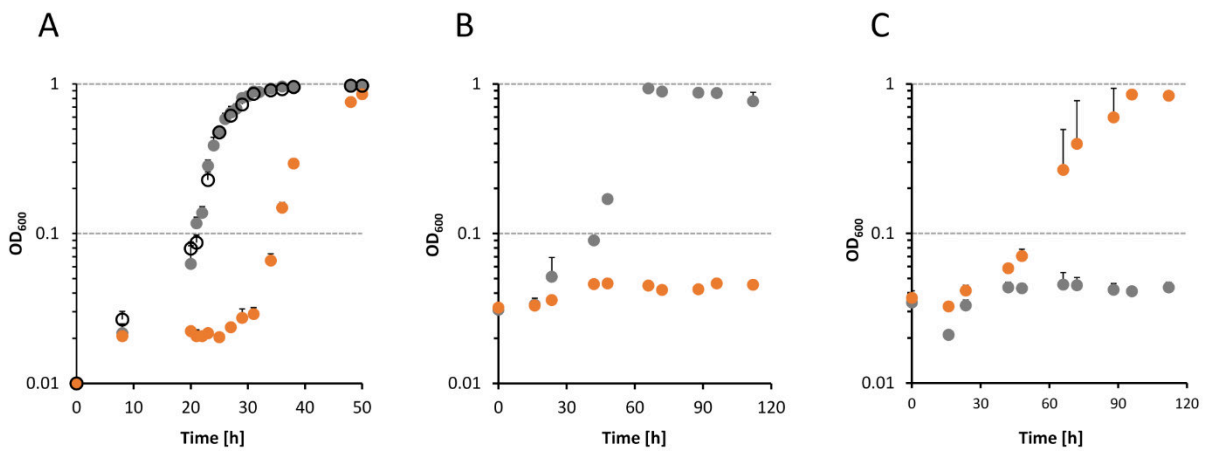

Figure 4: Growth of different *P. putida* strains at 30°C and 180 rpm shaking with M9 medium in polycarbonate Erlenmeyer flasks supplemented with 5 mM 2-phenylethanol and 10 µM La^{3+} in the absence (**A**) and presence of kanamycin (**B** and **C**) for plasmid maintenance. Flasks were inoculated at an OD_{600} of 0.01 (**A**) or 0.03 (**B** and **C**) with washed cells from M9 overnight cultures grown with succinate in the absence (**A**) or presence (**B** and **C**) of kanamycin and 0.2% rhamnose as inducer for the plasmids pJEM[PedR2] and pJEM[PedR2^{D53A}]. **A**) Growth of Δ*pedE* (black circles), Δ*pedE*_PedS2^{S178P} (orange dots), and Δ*pedE*_PedS2^{S178P}Δ*pedR2* (grey dots). **B**) Growth of Δ*pedH*_PedS2^{S178P}Δ*pedR2* harboring pJEM[PedR2] (grey dots) or pJEM[PedR2^{D53A}] (orange dots). **C**) Growth of Δ*pedE*_PedS2^{S178P}Δ*pedR2* harboring pJEM[PedR2] (grey dots) or pJEM[PedR2^{D53A}] (orange dots). Data points represent the mean of biological triplets and error bars correspond to the respective standard deviations (positive error values).

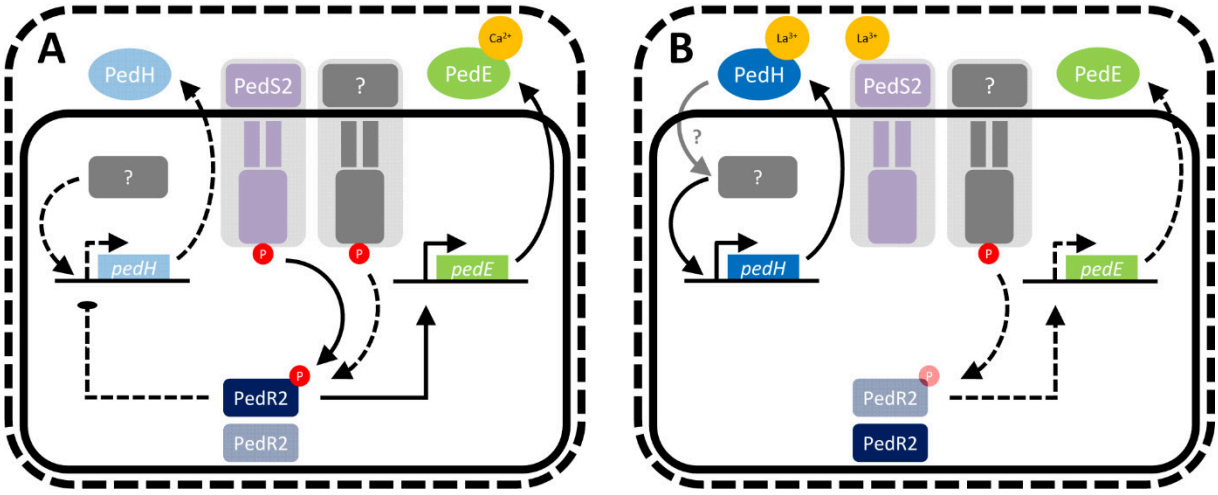

Figure 5: Working hypothesis of REE-mediated switch of *pedE* and *pedH* in *Pseudomonas putida* KT2440. Black lines indicate known regulations or functionalities. Grey boxes with question marks indicate unknown regulatory components. Solid lines indicate a strong regulatory effect on genes or production of enzymes, whereas dotted lines indicate weaker regulatory effects or low production of enzymes. A detailed description of the working model is given in the text.

443 # References

444 Agrawal, R., Sahoo, B.K., and Saini, D.K. (2016) Cross-talk and specificity in two-component
445 signal transduction pathways. *Future Microbiol.* **11**: 685–697.

446 Anthony, C. (2001) Pyrroloquinoline Quinone (PQQ) and Quinoprotein Enzymes. *Antioxid.*
447 *Redox Signal.* **3**: 757–774.

448 Arias, S., Olivera, E.R., Arcos, M., Naharro, G., and Luengo, J.M. (2008) Genetic analyses and
449 molecular characterization of the pathways involved in the conversion of 2-
450 phenylethylamine and 2-phenylethanol into phenylacetic acid in *Pseudomonas putida*
451 U. *Environ. Microbiol.* **10**: 413–432.

452 Bourret, R.B., Hess, J.F., and Simon, M.I. (1990) Conserved aspartate residues and
453 phosphorylation in signal transduction by the chemotaxis protein CheY. *Proc. Natl.*
454 *Acad. Sci.* **87**: 41–45.

455 Choi, K.-H., Gaynor, J.B., White, K.G., Lopez, C., Bosio, C.M., Karkhoff-Schweizer, R.R., and
456 Schweizer, H.P. (2005) A Tn7-based broad-range bacterial cloning and expression
457 system. *Nat. Methods* **2**: 443–448.

458 Chu, F., Beck, D.A.C., and Lidstrom, M.E. (2016) MxaY regulates the lanthanide-mediated
459 methanol dehydrogenase switch in *Methylomicrobium buryatense*. *PeerJ* **4**: e2435.

460 Chu, F. and Lidstrom, M.E. (2016) XoxF Acts as the Predominant Methanol Dehydrogenase in
461 the Type I Methanotroph *Methylomicrobium buryatense*. *J. Bacteriol.* **198**: 1317–1325.

462 van Dam, N.M., Weinhold, A., and Garbeva, P. (2016) Calling in the Dark: The Role of
463 Volatiles for Communication in the Rhizosphere. In, Blande,J.D. and Glinwood,R. (eds),
464 *Deciphering Chemical Language of Plant Communication*. Springer International
465 Publishing, Cham, pp. 175–210.

466 Farhan Ul Haque, M., Kalidass, B., Bandow, N., Turpin, E.A., DiSpirito, A.A., and Semrau, J.D.

467 (2015) Cerium Regulates Expression of Alternative Methanol Dehydrogenases in
468 *Methylosinus trichosporium* OB3b. *Appl. Environ. Microbiol.* **81**: 7546–7552.
469 Fitriyanto, N.A., Fushimi, M., Matsunaga, M., Pertiwiningrum, A., Iwama, T., and Kawai, K.
470 (2011a) Molecular structure and gene analysis of Ce3+ -induced methanol
471 dehydrogenase of *Bradyrhizobium* sp. MAFF211645. *J. Biosci. Bioeng.* **111**: 613–7.
472 Fitriyanto, N.A., Nakamura, M., Muto, S., Kato, K., Yabe, T., Iwama, T., et al. (2011b) Ce3+-
473 induced exopolysaccharide production by *Bradyrhizobium* sp. MAFF211645. *J. Biosci.*
474 *Bioeng.* **111**: 146–152.
475 Gibson, D.G. (2011) Enzymatic Assembly of Overlapping DNA Fragments. In, *Methods in*
476 *Enzymology*., pp. 349–361.
477 Good, N.M., Vu, H.N., Suriano, C.J., Subuyuj, G.A., Skovran, E., and Martinez-Gomez, N.C.
478 (2016) Pyrroloquinoline Quinone Ethanol Dehydrogenase in *Methylobacterium*
479 *extorquens* AM1 Extends Lanthanide-Dependent Metabolism to Multicarbon
480 Substrates. *J. Bacteriol.* **198**: 3109–3118.
481 Good, N.M., Walser, O.N., Moore, R.S., Suriano, C., Huff, A.F., and Martinez-Gomez, N.C.
482 (2018) Investigation of lanthanide-dependent methylotrophy uncovers complementary
483 roles for alcohol dehydrogenase enzymes. *bioRxiv*.
484 Graf, N. and Altenbuchner, J. (2011) Development of a method for markerless gene deletion
485 in *Pseudomonas putida*. *Appl. Environ. Microbiol.* **77**: 5549–5552.
486 Gu, W. and Semrau, J.D. (2017) Copper and cerium-regulated gene expression in
487 *Methylosinus trichosporium* OB3b. *Appl. Microbiol. Biotechnol.* **101**: 8499–8516.
488 Insam, H. and Seewald, M.S.A. (2010) Volatile organic compounds (VOCs) in soils. *Biol. Fertil.*
489 *Soils* **46**: 199–213.
490 Jeske, M. and Altenbuchner, J. (2010) The *Escherichia coli* rhamnose promoter rhaP BAD is in

491 *Pseudomonas putida* KT2440 independent of Crp–cAMP activation. *Appl. Microbiol.*
492 *Biotechnol.* **85**: 1923–1933.
493 Van Kessel, J.C., Rutherford, S.T., Shao, Y., Utria, A.F., and Bassler, B.L. (2013) Individual and
494 combined roles of the master regulators apha and luxr in control of the *Vibrio harveyi*
495 quorum-sensing regulon. *J. Bacteriol.* **195**: 436–443.
496 Letunic, I. and Bork, P. (2018) 20 years of the SMART protein domain annotation resource.
497 *Nucleic Acids Res.* **46**: D493–D496.
498 Lv, H., Sahin, N., and Tani, A. (2018) Isolation and genomic characterization of
499 *Novimethylophilus kurashikiensis* gen. nov. sp. nov., a new lanthanide-dependent
500 methylotrophic species of *Methylophilaceae*. *Environ. Microbiol.* **20**: 1204–1223.
501 Maniatis, T., Fritsch, E., Sambrook, J., and Laboratory, C.S.H. (1982) Molecular Cloning : A
502 Laboratory Manual Cold Spring Harbor, N.Y. Cold Spring Harbor Laboratory.
503 Masuda, S., Suzuki, Y., Fujitani, Y., Mitsui, R., Nakagawa, T., Shintani, M., and Tani, A. (2018)
504 Lanthanide-Dependent Regulation of Methylotrophy in *Methylobacterium aquaticum*
505 Strain 22A. *mSphere* **3**: e00462-17.
506 Mern, D.S., Ha, S.W., Khodaverdi, V., Gliese, N., and Gorisch, H. (2010) A complex regulatory
507 network controls aerobic ethanol oxidation in *Pseudomonas aeruginosa*: indication of
508 four levels of sensor kinases and response regulators. *Microbiology* **156**: 1505–1516.
509 Milani, M., Leoni, L., Rampioni, G., Zennaro, E., Ascenzi, P., and Bolognesi, M. (2005) An
510 active-like structure in the unphosphorylated StyR response regulator suggests a
511 phosphorylation-dependent allosteric activation mechanism. *Structure* **13**: 1289–1297.
512 Mückschel, B., Simon, O., Klebensberger, J., Graf, N., Rosche, B., Altenbuchner, J., et al.
513 (2012) Ethylene glycol metabolism by *Pseudomonas putida*. *Appl. Environ. Microbiol.*
514 **78**: 8531–9.

515 Nakagawa, T., Mitsui, R., Tani, A., Sasa, K., Tashiro, S., Iwama, T., et al. (2012) A Catalytic Role
516 of XoxF1 as La3+-Dependent Methanol Dehydrogenase in *Methylobacterium*
517 *extorquens* Strain AM1. *PLoS One* **7**: e50480.
518 Parkinson, J.S. (2010) Signaling Mechanisms of HAMP Domains in Chemoreceptors and
519 Sensor Kinases. *Annu. Rev. Microbiol.* **64**: 101–122.
520 Penuelas, J., Asensio, D., Tholl, D., Wenke, K., Rosenkranz, M., Piechulla, B., and Schnitzler,
521 J.P. (2014) Biogenic volatile emissions from the soil. *Plant. Cell Environ.* **37**: 1866–1891.
522 Pol, A., Barends, T.R.M., Dietl, A., Khadem, A.F., Eygensteyn, J., Jetten, M.S.M., and Op den
523 Camp, H.J.M. (2014) Rare earth metals are essential for methanotrophic life in volcanic
524 mudpots. *Environ. Microbiol.* **16**: 255–264.
525 Regenhardt, D., Heuer, H., Heim, S., Fernandez, D.U., Strompl, C., Moore, E.R.B., and Timmis,
526 K.N. (2002) Pedigree and taxonomic credentials of *Pseudomonas putid*a strain KT2440.
527 *Environ. Microbiol.* **4**: 912–915.
528 Rowland, M.A. and Deeds, E.J. (2014) Crosstalk and the evolution of specificity in two-
529 component signaling. *Proc. Natl. Acad. Sci.* **111**: 5550–5555.
530 Sarkar, B. (2002) Heavy Metals in the Environment CRC Press.
531 Schobert, M. and Görisch, H. (2001) A soluble two-component regulatory system controls
532 expression of quinoprotein ethanol dehydrogenase (QEDH) but not expression of
533 cytochrome c(550) of the ethanol-oxidation system in *Pseudomonas aeruginosa*.
534 *Microbiology* **147**: 363–372.
535 Semrau, J.D., DiSpirito, A.A., Gu, W., and Yoon, S. (2018) Metals and Methanotrophy. *Appl.*
536 *Environ. Microbiol.* **84**: e02289-17.
537 Shiller, A.M., Chan, E.W., Joung, D.J., Redmond, M.C., and Kessler, J.D. (2017) Light rare earth
538 element depletion during Deepwater Horizon blowout methanotrophy. *Sci. Rep.* **7**:

539 10389.

540 Sievers, F., Wilm, A., Dineen, D., Gibson, T.J., Karplus, K., Li, W., et al. (2014) Fast, scalable
541 generation of high-quality protein multiple sequence alignments using Clustal Omega.
542 *Mol. Syst. Biol.* **7**: 539–539.

543 Singh, V.S., Dubey, A.P., Gupta, A., Singh, S., Singh, B.N., and Tripathi, A.K. (2017) Regulation
544 of a Glycerol-Induced Quinoprotein Alcohol Dehydrogenase by σ 54 and a LuxR-Type
545 Regulator in *Azospirillum brasilense* Sp7. *J. Bacteriol.* **199**: e00035-17.

546 Skovran, E., Palmer, A.D., Rountree, A.M., Good, N.M., and Lidstrom, M.E. (2011) XoxF Is
547 Required for Expression of Methanol Dehydrogenase in *Methylobacterium extorquens*
548 AM1. *J. Bacteriol.* **193**: 6032–6038.

549 Springer, A.L., Auman, A.J., and Lidstrom, M.E. (1998) Sequence and characterization of
550 mxaB, a response regulator involved in regulation of methanol oxidation, and of mxaW,
551 a methanol-regulated gene in *Methylobacterium extorquens* AM1. *FEMS Microbiol. Lett.*
552 **160**: 119–24.

553 Springer, A.L., Morris, C.J., and Lidstrom, M.E. (1997) Molecular analysis of mxbD and mxbM,
554 a putative sensor-regulator pair required for oxidation of methanol in
555 *Methylobacterium extorquens* AM1. *Microbiology* **143**: 1737–1744.

556 Stock, A.M., Robinson, V.L., and Goudreau, P.N. (2000) Two-Component Signal Transduction.
557 *Annu. Rev. Biochem.* **69**: 183–215.

558 Taubert, M., Grob, C., Howat, A.M., Burns, O.J., Dixon, J.L., Chen, Y., and Murrell, J.C. (2015)
559 XoxF encoding an alternative methanol dehydrogenase is widespread in coastal marine
560 environments. *Environ. Microbiol.* **17**: 3937–3948.

561 Toyama, H., Mathews, F.S., Adachi, O., and Matsushita, K. (2004) Quinohemoprotein alcohol
562 dehydrogenases: structure, function, and physiology. *Arch. Biochem. Biophys.* **428**: 10–

563 21.

564 Vekeman, B., Speth, D., Wille, J., Cremers, G., De Vos, P., Op den Camp, H.J.M., and Heylen,
565 K. (2016) Genome Characteristics of Two Novel Type I Methanotrophs Enriched from
566 North Sea Sediments Containing Exclusively a Lanthanide-Dependent XoxF5-Type
567 Methanol Dehydrogenase. *Microb. Ecol.* **72**: 503–509.

568 Vu, H.N., Subuyuj, G.A., Vijayakumar, S., Good, N.M., Martinez-Gomez, N.C., and Skovran, E.
569 (2016) Lanthanide-Dependent Regulation of Methanol Oxidation Systems in
570 *Methylobacterium extorquens* AM1 and Their Contribution to Methanol Growth. *J.*
571 *Bacteriol.* **198**: 1250–1259.

572 Wackett, L.P. (2003) Pseudomonas putida- a versatile biocatalyst. *Nat. Biotechnol.*

573 Waters, C.M. and Bassler, B.L. (2006) The *Vibrio harveyi* quorum-sensing system uses shared
574 regulatory components to discriminate between multiple autoinducers. *Genes Dev.* **20**:
575 2754–2767.

576 Wehrmann, M., Billard, P., Martin-Meriadec, A., Zegeye, A., and Klebensberger, J. (2017)
577 Functional Role of Lanthanides in Enzymatic Activity and Transcriptional Regulation of
578 Pyrroloquinoline Quinone-Dependent Alcohol Dehydrogenases in *Pseudomonas putida*
579 KT2440. *MBio* **8**: e00570-17.

580 Winsor, G.L., Griffiths, E.J., Lo, R., Dhillon, B.K., Shay, J.A., and Brinkman, F.S.L. (2016)
581 Enhanced annotations and features for comparing thousands of *Pseudomonas* genomes
582 in the *Pseudomonas* genome database. *Nucleic Acids Res.* **44**: D646–D653.

583 Wu, X., Monchy, S., Taghavi, S., Zhu, W., Ramos, J., and van der Lelie, D. (2011) Comparative
584 genomics and functional analysis of niche-specific adaptation in *Pseudomonas putida*.
585 *FEMS Microbiol. Rev.* **35**: 299–323.

586 Xu, H.H., Janka, J.J., Viebahn, M., and Hanson, R.S. (1995) Nucleotide sequence of the mxcQ

587 and mxcE genes, required for methanol dehydrogenase synthesis in *Methylobacterium*
588 *organophilum* XX: a two-component regulatory system. *Microbiology* **141**: 2543–2551.
589 Zheng, Y., Huang, J., Zhao, F., and Chistoserdova, L. (2018) Physiological Effect of XoxG(4) on
590 Lanthanide-Dependent Methanotrophy. *MBio* **9**: e02430-17.
591